RF POWER MEASUREMENTS ON THE DIII-D GYROTRON INSTALLATION

K. Kajiwara,[1] J. Lohr, D. Ponce, and R.W. Callis

General Atomics, P.O. Box 85608, San Diego, California 92186-5608 USA
[1]ORISE, Oak Ridge, Tennessee, USA

e-mail: kajiwara@fusion.gat.com

The accurate measurement of the rf power injected into the tokamak is necessary for most plasma experiments. In the DIII-D facility, several different techniques are used to perform power measurements for each gyrotron pulse. The accuracy of calorimetric measurements of the generated power has been improved by development of a fitting function for analysis of the calorimetry signal. Measurements of the power transmitted to the tokamak are being made using a vacuum wave guide power monitor.

1. Introduction

Analysis of plasma physics experiments requires accurate measurements of the rf power injected into the tokamak from each gyrotron for each pulse. Power measurements have been made on DIII-D using calorimetric techniques to obtain the power loading of gyrotron components such as the output window, the cavity and the coupling optics. In principle, any of these measurements can be combined with *a priori* knowledge of gyrotron performance to determine the generated power. The measurement has been susceptible to errors due to the design of the water cooling system.

The DIII-D gyrotron cooling system is a large closed loop. All gyrotron cooling water circulates from a bank of pumps connected in parallel to the gyrotron manifolds, which are connected in parallel. A typical gyrotron operates at 30% electrical efficiency to generate about 800 kW of rf power, meaning that on each gyrotron pulse about 2.6 MW (mostly from the collector) is dissipated in the cooling circuits. Simultaneous 2 s pulses from six gyrotrons release 32 MJ of heat to a volume of water, which circulates back to the reservoir and is returned, more or less coherently, to the gyrotron manifolds. The total volume of the gyrotron cooling water is 5.3×10^4 liters and the total gyrotron cooling water flow is 1.1×10^4 liters per minute. The efficiency of the heat exchanger system is 15%–75% which depends on the condition of filters and the heat exchanger itself. In this cooling system, the mixing is poor and the temperature of water delivered to the gyrotrons can fluctuate. To eliminate the inaccuracy of the power measurements related to water temperature fluctuation, a fitting function has been developed which permits an analytical treatment of the calorimetry response to be made. In Sec. 3, the fitting function and fitting results are reported.

2. Calorimetry Analysis

Figures 1(a) through (d) show typical waveforms for the temperature measurements of gyrotron cooling water (2 s pulse width with ~800 kW rf power generation) and the estimated power during 2003 DIII-D operations. The power injected into the plasma is calculated using the following formula,

$$P_{inj} = \left(P_{cav}/\alpha - P_{MOU}\right) \times \Psi \quad . \tag{1}$$

Here, P_{cav} and P_{MOU} indicate the rf power loss at the gyrotron cavity and the Matching Optics Unit (MOU), respectively. The symbol α is ratio of the cavity power loading at the cavity to the total output power of the gyrotron, which was measured during testing at the manufacturer and Ψ is the transmission efficiency. As shown in Figs. 1(a) and (b), fluctuations in ΔT, the temperature difference between the input and output water, reached ~10% for a 2 s pulse, which contributes to measurement error because of the difficulty of determining the base line. In typical DIII-D gyrotron operation, the ΔT fluctuations resulting from baseline fluctuations are about 0.04ºC, which causes ±10% power measurement error for the cavity and ±15% error for the MOU, for 2 s and 800 kW, as shown in dashed lines in Fig.1(c,d). To eliminate this error, an analytical function to fit the time dependence of the difference signal has been developed.

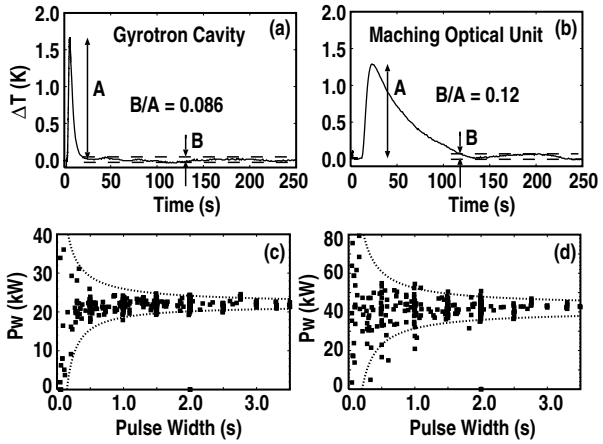

Figure 1. Typical wave forms of the temperature measurement of the cooling water for (a) cavity and (b) MOU (2 s and 800 kW pulse). The vertical axis shows ΔT which is the temperature difference of the input and output water. Figures (c) and (d) show the estimated powers as a function of the gyrotron pulse width for cavity and MOU, respectively. The power is calculated by the time integration of ΔT. The data in (c) and (d) include all 2003 DIII-D gyrotron plasma injection. The dashed line in (c) and (d) shows the possible error by the 0.04°C temperature fluctuation of the water.

Figure 2 shows the cooling model for the fitting function. For simplicity, the model is zero dimensional. We assume that the rf heats all of the water-cooled material and that there is no heat diffusion through the cooling water, which would distort the ΔT time dependance, or through the structural supports. The equations are as follows:

If $0 > t < t_p$,

$$\begin{cases} C_C \dfrac{dT_{C1}(t)}{dt} = -\alpha_{wC} S_C \left[T_{C1}(t) - T_{w0}\right] + P_w \\ C_D \dfrac{dT_{D1}(t)}{dt} = \alpha_{wD} S_D \left\{ \dfrac{\alpha_{wC} S_C \left[T_{C1}(t) - T_{w0}\right]}{C_w} + T_{w0} - T_{D1}(t) \right\} \\ T_{D1}(0) = T_{w0},\ T_{C1}(0) = T_{w0} \end{cases} . \quad (2)$$

If $t < t_p$,

$$\begin{cases} C_C \dfrac{dT_{C2}(t)}{dt} = -\alpha_{wC} S_C \left[T_{C2}(t) - T_{w0}\right] \\ C_D \dfrac{dT_{D2}(t)}{dt} = \alpha_{wD} S_D \left\{ \dfrac{\alpha_{wC} S_C \left[T_{C2}(t) - T_{w0}\right]}{C_w} + T_{w0} - T_{D2}(t) \right\} \\ T_{D2}(t_p) = T_{D1}(t_p),\ T_{C2}(t_p) = T_{C1}(t_p) \end{cases} . \quad (3)$$

Here, $C_C = \rho C_{Cu} V_C / m_c$ (J/K), $C_D = \rho C_{Cu} V_D / m_c$ (J/K), $C_w = C_{H_2O} f \times 3785$ (g)/60 (s) (J/K), and t_p is the gyrotron pulse width. The symbols ρ, C_{Cu}, V_C, V_D and m_c are the density of copper (kg m^{-3}), the specific heat of copper (JK^{-1} mol^{-1}), the volume of cooled material (m^3), the volume of the detector (only a part of the detector is immersed in the water in the water) (m^3) and the atomic number of copper (g mol^{-1}), respectively. The parameters C_{H_2O} and f show the specific heat of water (J/K/g) and flow (gpm). The $T_C(t)$, $T_D(t)$, S_C and S_D are temperatures of the water-cooled material, the temperature of the detector, the surface area of water cooled material (m^2), and the surface area of the detector (m^2), respectively. The heat transfer coefficient (Wm^{-2} K^{-1}) between the water and the water cooled material, and the water and the detector are indicated by α_{wC} and α_{wD}, respectively. Equations (2) and (3) can be solved analytically. The analytical solution is in Appendix A. By using the analytical solution, the whole temperature signal could be fitted by T_{D1} and T_{D2} as functions of time. The fitting parameters are P_w, α_{wC} and α_{wD}.

The fitting algorithm is the nonlinear least-squares (NLLS) Marquardt-Levenberg algorithm. Here, the fitting parameters α_{wD} and α_{wC} are affected by cooling water temperature fluctuations. However, we can estimate α_{wD} and α_{wC} by accumulating data from many gyrotron pulses, especially pulses longer than 3 s to average over the fluctuations. The accumulated data shows the typical α_{wD} and α_{wC} are 2090 and 1810 for the cavity and 1660 and 680 ($Wm^{-2}K^{-1}$) for the MOU, respectively. The especially low value of α_{wC} for the MOU is caused by the assumption of no heat diffusion in the cooling water. The water flow for the MOU is much smaller than for the cavity, which increases the heat diffusion during the transit of water though the MOU. Using these heat transfer coefficients, the estimated power is shown as Fig. 3(c,d). The power measurement errors are reduced from ±10% to ±6% for the cavity and from ±15% to ±7% for the MOU for 2 s pulses. By comparing Fig. 1(c,d) and Fig. 3(c,d), one concludes that the fitting method provides the greatest increase in accuracy for short pulses. There is no significant advantage for the fitting method unless the pulse width becomes >0.5 s. The figures also show the method is more useful for slow flow velocity circuits such as the MOU.

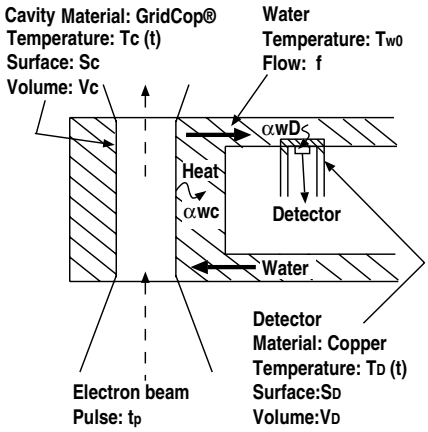

Figure 2: Water-cooling model for gyrotron cavity..

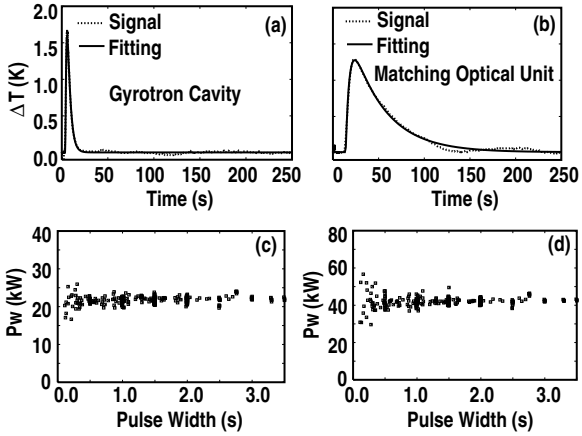

Figure 3 Fitting result for (a) cavity and (b) MOU. Figure (c) and (d) show the estimated powers by a fitting method with the assumption of α_{wD} and α_{wC} are 2090 and 1810 for cavity and 1660 and 680 ($Wm^{-2}K^{-1}$) for MOU, respectively. The gyrotron shots including Fig. 1(c) and (d) are all included.

Figure 4 shows another important advantage of the fitting method. If the ΔT signal is arbitrarily truncated 15 s after the peak the fitting function still provides similar accuracy as the non-truncated signal, as shown in Fig. 4(a). The estimated power is shown in Fig. 4(b) which is almost identical with Fig. 3(d). This becomes important during plasma experiments when there is limited time between tokamak shots during which to acquire calorimetry data or gyrotron conditioning is required.

3. Built-in Waveguide Power Monitor

For measurements of the rf power delivered to the plasma, a built-in wave guide power monitor was developed. Figure 5 shows the schematic view of the power monitor. A small gap in the corrugated waveguide transmission line is covered by a thin wall stainless steel cylinder with a band of TiO_2 plasma sprayed on the inside of the cylinder adjacent to the gap. The rf power leaking from the gap is absorbed by the TiO_2. The radial heat diffusion from the TiO_2 through the stailnless steel is much faster than diffusion in the axial direction. Therefore, the peak temperature of the outside of the cylinder at the TiO_2 is proportional to the leakage rf power, which is proportional to the power in the waveguide. Figure 6 shows the typical time dependance of the temperature increase on the outside of the cylinder. There is a sharp temperature increase as expected.

A calibration of the temperature increase per unit power in the waveguide is performed using a long waveguide line. The length and

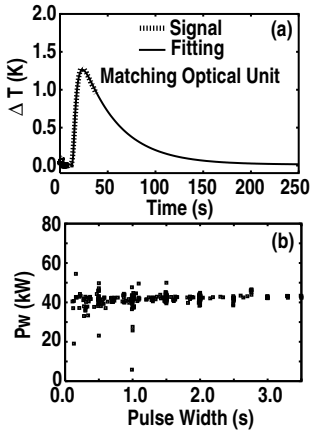

Figure 4: (a) The ΔT signail is arbitrarily truncated 15 s after the peak. Figure (b) shows the estimated powers by a fitting method with the artificially truncated signals.

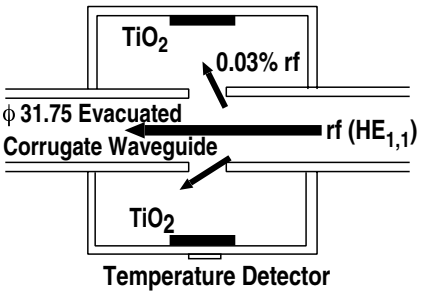

Figure 5: Schematic view of the built-in wave guide power monitor.

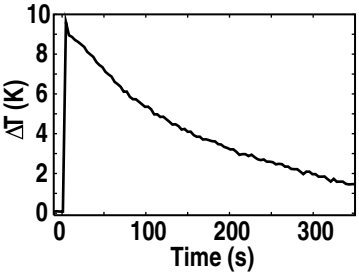

Figure 6: Typical temperature increase of the built-in power monitor.

number of miter bends in the test line approximates an actual DIII-D transmission line, including two polarizing miters, which are located close to the gyrotron. At a specific azimuthal position on the cylinder, the peak temperature increase is found to have a dependence on the polarization direction with respect to the plane of the miter bend, as shown in Fig. 7. Four resistance temperature devices (RTD) are attached 90 deg apart around the circumference of the cylinder. In pite of the long waveguide run (~80 m) between the gyrotron and the monitor, which should filter higher order waveguide modes, there is a strong dependence of the temperature on azimuth. Since, the rotation of the polarizing miter rotates the elliptical polarization of the traveling wave, low order undesired modes such as HE_{1n}, TE_{01}, TM_{02} and HE_{21} are expected to rotate with the polarizer andyield a symmetric temperature configuration, unlike the observation. The asymmetric temperature increase as shown in RTD1 and RTD3 suggests that these temperatures are influenced by a complex mixture of undesired modes. An empirical calibration of response as a function of polarization direction and ellipticity in the actual transmission line is required.

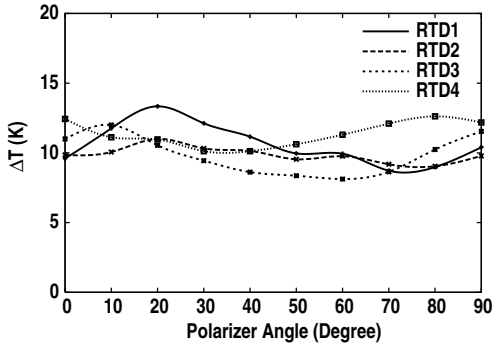

Figure 7: Typical temperature increase of the built-in power monitor as a function of the wave polarization,

4. Summary

The two methods have been used to measure the ECH power in the DIII-D installation. The first is the usual calorimetric power measurement where the gyrotron generated power is estimated from the power loading of the gyrotron cavity for plasma injection. This method suffers from water temperature fluctuation, typically $\Delta T \sim 0.04°C$, in the DIII-D installation. These fluctuations cause ±10% power measurement errors for 2 s, 800 kW pulses typically used in experiments. The error is reduced to ±6% by developing a fitting function for the $\Delta T(t)$ signal. The second method is based on a leaky waveguide power monitor. The power monitor has been tested with a long transmission line (~80 m) for various directions of the electric field of the traveling wave. The results show the monitor is very sensitive to the polarization direction, indicating that calibrations for a range of polarization directions in the actual transmission line is required.

Acknowledgment

Work supported by the U.S. Department of Energy under DE-FC02-04ER54698 and DE-AC05-76OR00033.